Angiogenesis
https://doi.org/10.1007/s10456-024-09944-6

ORIGINAL PAPER

The angiogenic role of the alpha 9-nicotinic acetylcholine receptor in triple-negative breast cancers

Sonjid Ochirbat[1] · Tzu-Chun Kan[2,3] · Chun-Chun Hsu[2,4,5] · Tzu-Hsuan Huang[2,6] · Kuo-Hsiang Chuang[7] · Michael Chen[7] · Chun-Chia Cheng[8] · Chun-Chao Chang[9,10,11] · Sri Rahayu[12] · Jungshan Chang[1,2,13]

Received: 5 March 2024 / Accepted: 19 August 2024
© The Author(s), under exclusive licence to Springer Nature B.V. 2024

Abstract

Nicotine acts as an angiogenic factor by stimulating endogenous cholinergic pathways. Several subtypes of nicotinic acetylcholine receptors (nAChRs) have been demonstrated to be closely correlated to the formation and progression of different types of cancers. Recently, several studies have found that nicotinic acetylcholine receptors α9 (α9-nAChRs) are highly expressed in breast tumors, especially in tumors derived from patients diagnosed at advanced stages. In vitro studies have demonstrated that activation of α9-nAChRs is associated with increased proliferation and migration of breast cancer. To study the tumor-promoting role of α9-nAChRs in breast cancers, we generated a novel anti-α9-nAChR and methoxy-polyethylene glycol (mPEG) bispecific antibody (α9 BsAb) for dissecting the molecular mechanism on α9-nAChR-mediated tumor progression. Unexpectedly, we discovered the angiogenic role of α9-nAChR in nicotine-induced neovascularization of tumors. It revealed α9 BsAbs reduced nicotine-induced endothelial cell tube formation, blood vessel development in Matrigel plug assay and angiogenesis in microtube array membrane murine model (MTAMs). To unbraid the molecular mechanism of α9-nAChR in nicotine-mediated angiogenesis, the α9 BsAbs were applied and revealed the inhibitory roles in nicotine-induced production of hypoxia-inducible factor-2 alpha (HIF-2α), vascular endothelial growth factor A (VEGF-A), phosphorylated vascular endothelial growth factor receptor 2 (p-VEGFR2), vascular endothelial growth factor receptor 2 (VEGFR2) and matrix metalloproteinase-9 (MMP9) from triple-negative breast cancer cells (MDA-MB-231), suggesting α9-nAChRs played an important role in nicotine-induced angiogenesis. To confirm our results, the shRNA targeting α9-nAChRs was designed and used to silence α9-nAChR expression and then evaluated the angiogenic role of α9-nAChRs. The results showed α9 shRNA also played an inhibitory effect in blocking the nicotine-induced angiogenic signaling. Taken together, α9-nAChR played a critical role in nicotine-induced angiogenesis and this bispecific antibody (α9 BsAb) may serve as a potential therapeutic candidate for treatments of the α9 positive cancers.

Keywords Nicotine · Nicotinic acetylcholine receptors α9 · Bispecific antibody · Angiogenesis · Microtube array membrane murine model

Introduction

Development and growth of tumors strictly require an abundant supply of nutrients and oxygen from newly formed blood vessels [1]. Therefore, the formation of new blood vessels is referred to as an angiogenesis which is involved in the collected actions and processes of migration, growth and development of endothelial cells (ECs). Interruption or blockage of angiogenesis is considered one of the therapeutic strategies for cancer patients. Previous studies have indicated that vascular endothelial growth factors (VEGFs) and their receptors (VEGFRs) are considered as the most critical pro-angiogenic factors in regulating tumor angiogenesis [2–4]. In the classical paracrine signaling pathway, tumor-derived VEGF interacts with VEGFR2 on neighboring ECs, leading to prolonged survival, proliferation, migration, and development of ECs through the activation of several key intermediate regulators in the VEGF-VEGFR2 axis and downstream signaling pathways such as focal adhesion kinase (FAK), Src, extracellular-signal-regulated kinase (ERK)1/2, and Akt, which is resulted in angiogenesis [1]. In addition to the constitutive expression of VEFGRs on ECs, VEGFR2 is also expressed on various forms of cancer cells including breast cancer [5–9], lung cancer [10], glioblastoma [11],

Extended author information available on the last page of the article

Published online: 23 August 2024

gastrointestinal cancer [12], bladder cancer [13], hepatocellular carcinoma, renal cell carcinoma [14], ovarian cancer [15] and osteosarcoma [16]. Therefore, VEGF-A secreted from cancer cells binds to VEGFR2 on their own cell surface resembling as an autocrine loop, promoting themselves on growth and survival [17].

It has been well known that nicotine is considered as an agent for angiogenesis. Nicotine induces angiogenesis in a number of settings including ischemia, inflammation, age-related macular degeneration, atherosclerosis and cancers [18]. This nicotine-induced pro-angiogenic activity is mediated through the interaction of nicotinic acetylcholine receptors (nAChRs) expressed on ECs [19].

nAChRs belong to the ligand-gated ion channel superfamily of neurotransmitter receptors and their expressions were found throughout the entire body [20]. These receptors consist of 5 subunits and each subunit exists as 16 isoforms (α1–α10, β1–β4, δ, γ and ε), arranging either in hetero- or homo-pentameric configuration [21]. The combinations of various α- and β- subunits result in functionally multiple nAChR subtypes that behave differently in terms of ion permeability, open time, ligand affinity and other functions. These nAChRs are expressed on venous, lymphatic, arterial or microvascular ECs equipped with possibly different subtypes or proportions of subtypes, contributing to display similar or divergent functions [22]. In addition, nicotine also binds nAChRs on several types of cancer cells and activates nAChR-mediated down signaling, promoting cell migration, proliferation and survival [23, 24].

Although nicotine is not considered as a carcinogenic agent, it exerts oncogenic effects such as angiogenesis and tumor growth via cholinergic pathway [18]. Moreover, an increased expression of VEGF-A and VEGFR2 in several types of cancer cells exposed to nicotine was observed, suggesting nicotine possesses pro-angiogenic potential [25, 26]. The pharmacological inhibition or genetic disruption of α7-nAChR expression reversed nicotine-mediated proangiogenic effects in endothelial cells, indicating α7-nAChRs played a dominant role in mediating nicotine-induced angiogenesis [18, 19]. Nevertheless, other endothelial subunits have not been functionally characterized yet. Currently, the roles of homo-pentameric alpha 9 subtype of nAChRs (α9-nAChR) in breast cancers have been carefully investigated. An epidemiological cohort study demonstrated that α9-nAChR mRNA level in breast tumor tissues was 7.84-fold higher than in surrounding normal tissues and this occurred more often in smokers. In addition, the authors discovered that higher α9-nAChR expression was more frequently observed in advanced-stage (stages 3 and 4) breast cancer tissues and was associated with a poor 5-year disease-specific survival rate [27]. Further research studies demonstrated that nicotine induced significantly higher expression of α9-nAChRs in breast cancer cells [28]. Recently, it also revealed that nicotine promoted migration, invasion, proliferation and survival of various cancers including lung cancers, breast cancer and melanoma via α9-nAChR-mediated multiple downstream signaling pathways [27, 29–32]. It suggests that α9-nAChRs play an important role in nicotine-mediated tumor progression. However, the role of α9-nAChRs in angiogenesis remains unclear.

In this study, we assessed the role of α9-nAChR in angiogenesis coupled with the putative molecular mechanism using the novel bispecific monoclonal antibodies against α9-nAChR and methoxy polyethylene glycol (mPEG) (α9 BsAb). Our results indicated that α9 BsAb blocked nicotine-induced angiogenesis in three typical models for angiogenesis assessment including the tube formation assay, the Matrigel plug assay and the Microtube Array Membrane Hollow Fiber (MTAM-HFA) assay. We also found that nicotine-induced activation of α9-nAChR triggered productions of HIF-2α, VEGF-A, p-VEGFR2, VEGFR2 and MMP9 in MDA-MB-231 cells and this nicotine-mediated upregulated molecular signaling was blocked by α9 BsAb and anti-α9 shRNA. In addition to α7-nAChRs, we revealed α9-nAChRs as a new member of acetylcholine receptors play an important role in nicotine-induced angiogenic role in cancers. Moreover, α9 BsAb can be conjugated with Liposomal Doxorubicin (Lipo-Dox) and form antibody–drug conjugates (ADC) as α9 BsAbs-liposomal doxorubicin (α9 BsAbs/Lipo-Dox) to improve therapeutic efficacy for treatments of α9-nAChR positive cancers in the future.

Materials and methods

Cell lines and cell cultures

Human breast cancer cells and primary human umbilical vein endothelial cells (HUVECs) were used in this study according to the manufacturer's instructions.

The human breast cancer cell lines; luminal-type (MCF7) and TNBC-type (MDA-MB-231), were purchased from American Type Culture Collection (ATCC, Manassas, VA, USA). The breast cancer cells were grown in Dulbecco's Modified Eagle Medium/Nutrient Mixture F-12 medium (DMEM/F12; Thermo Fisher Scientific Inc., Waltham, MA, USA) supplemented with 10% heat-inactivated fetal bovine serum (FBS; Thermo Fisher Scientific Inc., Waltham, MA, USA) and 1% penicillin–streptomycin solution (HyClone™ 100X solution; Cytiva, Marlborough, MA, USA).

HUVECs were purchased from Promocell (#C12200, Heidelberg, Germany). Endothelial Cell Growth Medium contained Endothelial Cell Growth Supplement (Promocell, Heidelberg, Germany) was mixed with 10% FBS and 1% penicillin–streptomycin solution and used to culture

HUVECs on gelatin-coated dishes. HUVECs at passages from 3 to 5 were used for performing experiments.

Both cell cultures were maintained in a 5% CO_2 humidified incubator at 37 °C.

The preparation of bispecific antibody

Based on the DNA sequence encoding α9-nAChR scFv from Dr. Yi-Yuan Yang's team, Dr. Kuo-Hsiang Chuang's team constructed anti-α9-nAChR and anti-mPEG bispecific antibody (α9 BsAb) by genetic engineering with minor modification as described in their previous work [33]. Briefly, the light chain and heavy chain of humanized anti-mPEG Fab were genetically linked with an internal ribosome entry site (IRES) for co-expressing in a single plasmid. The Fv fragment of anti-α9-nAChR was genetically linked after the heavy chain of humanized anti-mPEG Fab. This chimeric gene construct of α9 BsAb was produced by transient transfection of pLNCX plasmid into Expi293 mammalian cell expression. α9 BsAb at a concentration of 1.1 mg/ml is prepared by diluting with PBS + 0.05% bovine albumin serum (BSA) and stored at −20 °C.

The collection of conditioned medium

The breast cancer cells were seeded in 6-well plates with 5×10^5 cells/well density. Next, cells were treated with α9 BsAb (0.7, 7, 14 μg/ml) and nicotine (0.1, 1, 10, 100 μM) for 72 h and then media were collected. To remove cell debris, the collected media were centrifuged for 10 min at 10,000 rpm and 4 °C. The supernatants were derived and used as conditioned medium. The conditioned medium was stored in a refrigerator at −80 °C for subsequent experiments.

Tube formation assay

Tube formation assay was performed on HUVECs using a μ-Slide (ibidi, Martinsried, Germany). Growth Factor Reduced Matrigel® Matrix (Cat. 356231; Corning Inc., New York, NY, USA) was thawed overnight at 4 °C. Using cold pipette tips, 10 μl of Growth Factor Reduced Matrigel was applied into the inner well of the μ-Slide. Following the polymerization of Matrigel in an incubator at 37 °C for 30 min, 50 μl of loading suspension was placed in the upper well of the μ-Slide. The loading suspension was prepared by mixing HUVECs (1×10^4 cells/well), α9 BsAb (0.7, 7, 14 μg/ml) and nicotine (10 μM) in Endothelial Cell Growth Medium. Then, μ-Slides were placed in an incubator at 37 °C with 5% CO_2 for 8 h. Images of the wells were taken using an inverted microscopy at 4× magnification. The number of loops formed in each well was counted for analysis.

Transwell assays

The migration efficacy of MDA-MB-231 cells was investigated using 8 μm Transwell inserts (Corning, NY, USA). 1×10^5 cells/well were seeded in the inner part of the insert filled with 300 μl of serum-free medium containing 10 μM nicotine and different concentrations of α9 BsAb (0.7, 7, 14 μg/ml). The outer part of the inserts was filled with 750 μl of complete culture medium. After 12 h of incubation at 37 °C with 5% CO_2, the medium was carefully removed from the inserts and the inserts were washed twice with PBS. The migrated cells were fixed on the inserts in 100% methanol for 20 min at room temperature. To stain the migrated cells, 750 μl of 0.2% crystal violet was added to each well of the 24-well plates and the inserts with fixed cells were placed inside. Following the staining step, the inserts were rinsed with distilled water to eliminate the excess crystal violet and the non-migrating cells on the upper surface of the insert were carefully removed with a cotton swab. The stained membranes were then cut out from the inserts using a surgical scalpel and mounted on a glass slide with glycerol gelatin. Five fields (center, north, south, west and east) of each membrane mounted on slides were randomly selected and their images were captured under the inverted microscope at 20× magnification.

For the invasion assay, 0.1 ml of Growth Factor Reduced Matrigel matrix (Corning, Tewksbury, MA, USA) diluted in buffer, extracellular matrix (ECM) materials was added to the transwell inserts for coating and placed in the incubator at 37 °C for 2 h to solidify. The remaining steps were the same as for the migration assay.

Enzyme-linked immunosorbent assay (ELISA)

Using a human VEGF ELISA kit (Bioss; Woburn, Massachusetts, USA), the VEGF concentration was measured in the conditioned medium derived from the supernatant of MDA-MB-231 cells. According to the manufacturer's protocol, 100 μl of standards or samples were pipetted into 96-well microplates pre-coated with VEGF monoclonal antibodies and incubated at 37 °C for 1 h 30 min. Afterward, the unbound samples were removed during a wash step, and then the biotinylated VEGF antibody was added to the wells. Following an hour of incubation, the unbound detection antibody was washed off and streptavidin solution conjugated with the enzyme horseradish peroxidase (HRP) was added to the wells. After subsequent incubation and wash steps, a 3,3',5,5'-tetramethylbenzidine (TMB) substrate solution to detect HRP activity was added, resulting in a blue-colored product presented proportionally to the amount of VEGF in the samples was formed. The reaction was terminated by the addition of a stop solution. The absorbance was measured at 450 nm using the μQuant™ Universal Microplate

Spectrophotometer (BioTek, Winowski, VT, USA). The VEGF concentration in the sample was estimated from a standard curve generated by making serial dilutions of the stock solution (human VEGF standard 2000 pg/ml).

Western blotting

MDA-MB-231 cells were treated with different concentrations of α9 BsAb (0.7, 7, 14 μg/ml) and nicotine (0.1, 1, 10, 100 μM) for different periods of time. Treated cells were washed twice with ice-cold PBS and lysed overnight at −20 °C in RIPA (Sigma-Aldrich) supplemented with phosphatase and protease inhibitors. After collecting protein samples through centrifugation at 12,000 rpm for 30 min at 4 °C, a standard curve was generated with 2 mg/ml bovine serum albumin (BSA) to determine the protein concentrations of the samples. Equal amounts of proteins were separated electrophoretically on polyacrylamide gels with sodium dodecyl sulfate and then transferred to polyvinylidene difluoride membranes (Millipore, CA, USA). The membranes were blocked in 3% BSA for an hour and kept overnight at 4 °C with the following specific primary antibodies. CHRNA9 (ARG55213; Arigo, Glasgow, UK), VEGF-a (Sc-7269; Santa Cruz Biotechnology, TM, US), VEGFR2 (2472; Cell Signaling Technology, Danvers, MA, USA), phospho-VEGFR2 (Tyr1175) (2478; Cell Signaling Technology, Danvers, MA, USA), HIF-2 alpha (NB100-122; Novus Biologicals, Centennial, CO, USA), MMP2 (A6247; ABclonal, Biotech Co., Ltd., Woburn, MA, USA), MMP9 (A0289; ABclonal, Biotech Co., Ltd., Woburn, MA, USA) and GAPDH (GTX100118; GeneTex, Irvine, CA, USA). The primary antibodies were probed with horseradish peroxidase (HRP) conjugated anti-mouse (Cat. A9044, Sigma-Aldrich, Burlington, VT, USA) or anti-rabbit (Cat. SI-A0545; Sigma-Aldrich, Burlington, VT, USA) secondary antibodies. Signals were detected with a chemiluminescent reagent (Millipore Corporation, Billerica, MA 01821 USA) using the ChemiDoc system (Bio-Rad Laboratories, Hercules, CA, USA) and semi-quantification was performed with the Image Lab System (Bio-Rad Laboratories, Hercules, CA, USA).

Quantitative real-time PCR (qRT-PCR)

RNA extraction and synthesis of complementary DNA (cDNA) were performed using the GENEzol™ TriRNA Pure Kit (Geneaid, New Taipei City, Taiwan) and the ToolsQuant II Fast RT Kit (BIOTOOLS Co., Ltd., New Taipei City, Taiwan), respectively. The purity of total RNA and the concentration of cDNA were determined using the Nanodrop spectrophotometer (ND 1000, Thermo Scientific). A reaction mixture with a final volume of 20 μl was prepared in a PCR tube containing 10 μl iTaq™ Universal SYBR® Green Supermix (Bio-Rad, Hercules, CA, USA), 5 μl template cDNA (10 ng/μl), 3 μl RNase-free water and 10 μM forward and reverse primers. The following specific primer pairs were targeted to CHRNA9 (Forward: AAA GAT GAA CTG GTC CCA TTC CT; Reverse: AAG GTC ATT AAA CAA CTT CTG AGC ATA T), VEGF-a (Forward: AGG AGG AGG GCA GAA TCA TCA; Reverse: CTC GAT TGG ATG GCA GTA GCT), VEGF-b (Forward: AAG GAC AGT GCT GTG AAG CCA G; Reverse: TGG AGT GGG ATG GGT GAT GTC A), VEGF-c (Forward: GCC AAT CAC ACT TCC TGC CGA T; Reverse: AGG TCT TGT TCG CTG CCT GAC A) and GAPDH (Forward: CAT CAC TGC CAC CCA GAA GAC TG; Reverse: ATG CCA GTG AGC TTC CCG TTC AG). The qPCR conditions were set as 95 °C for 30 s (polymerase activation and DNA denaturation), followed by 40 cycles of 95 °C for 5 s (denaturation), and 60 °C for 30 s (annealing/extension) using the QIAGEN Rotor-Gene Q machine. The expression level of the gene of interest was quantified using the Livak (ΔΔCt) method and compared with the level of the internal control GAPDH in all samples.

shRNA Plasmid stable transfection

In order to establish a stable knockdown of α9-nAChR expression in MDA-MB-231 cells, shRNA clones were purchased from the National RNAi Core Facility Platform (RNAi Core, Academia Sinica, Taipei, Taiwan). Plasmid DNA was then isolated using a Wizard® Plus SV Minipreps DNA Purification System (Promega, Madison, WI, USA) according to the manufacturer's protocol. Prior to transfection, 293 T cells were seeded overnight in a culture medium. The next day, the cells were transfected with plasmid DNA, the lentiviral packaging plasmid (pCMV-dR8.91) and the envelop plasmids (pMD2.G) using PolyJet in vitro DNA transfection reagent (SignaGen, Frederick, MD, USA) in accordance with the manufacturer's recommended protocol. After 12 h, the medium was replaced with a culture medium to allow continuous production of the virus. Viral supernatants were harvested after 48 h and filtered through a 0.45 μm filter before either being used for transduction or stored in a refrigerator at − 80 °C. Transduction of MDA-MB-231 cells was performed by incubating the cells with the viral supernatant in the presence of 10 μg/ml polybrene for 48 h. Finally, the stably transduced cells were selected and cultured by adding 2 μg/ml puromycin (Invivogen, San Diego, CA, USA) in the culture medium.

Mice and housing condition

Female NOD.Cg-PrkdcscidIl2rgtm1Wjl/SzJ (NSG) and C57BL/6 mice at 4 to 6 weeks of age were purchased from the National Laboratory Animal Center (Taipei, Taiwan).

Upon arrival at our institute, the mice were allowed to be adopted in the animal housing room for one week before the experiments began. The mice were housed in groups of five, in standard transparent Makrolon cages, under 12-h light–dark cycle with ad libitum feeding at the Laboratory Animal Center of Taipei Medical University.

All procedures performed on the animal models in this study were approved by the Taipei Medical University (TMU) Institutional Animal Care and Use Committee (IACUC No. LAC-2021-0546).

Microtube array membranes (MTAMs)

The establishment of Microtube Array Membranes (MTAMs; Bioman Scientific Co., Ltd, New Taipei City, Taiwan) was carried out on C57BL/6 mice. First, a cell suspension in 10 µl PBS at a density of 1×10^6 MDA-MB-231 cells was loaded into sterile MTAMs via capillary motion and both ends of the MTAMs were folded with a forcep. After loading cells, the MTAMs were placed in culture dishes with culture medium and incubated at 37 °C and 5% CO_2 for 24 h. Before implantation, the cell-loaded MTAMs were rinsed with autoclaved PBS buffer to remove residual media. Under inhalation of 3% isoflurane, the following surgical procedures were performed on mice. The mice were prepared by shaving their backs and then 5 mm length of incisions were made on both sides of the spinal column. After mucus layers were separated from the underlying flesh with surgical scissors, the cell-loaded MTAMs were implanted subcutaneously using laboratory spatulas and the wound site was then closed with sutures. 3 d after acclimatization, the mice were randomly divided into two groups and injected weekly with PBS buffer (5 ml/kg) and α9 BsAb (0.42 mg/kg) through the tail vein. 14 d after the start of the treatments, the mice were sacrificed and their dorsal skin was surgically opened to photograph the membranes together with a scale ruler under a dissecting microscope.

Matrigel plug angiogenesis assay

Matrigel plug assay was performed in NOD.Cg-PrkdcscidIl-2rgtm1Wjl/SzJ (NSG) mice. To prepare the Matrigel mixture, 2×10^6 MDA-MB-231 cells suspended in PBS were mixed with ice-cold Growth Factor Reduced Matrigel® Matrix in the same volume ratio. Under inhalation anesthesia with isoflurane, the mice were injected subcutaneously with a volume of 500 µl of the Matrigel mixture (day 0). After polymerization and formation of the gel plug, the mice were randomly divided into 3 groups: PBS buffer (I), nicotine (II) and nicotine + α9 BsAb (III). Animals were received nicotine (200 µg/ml) from day 0 to 14 in their drinking water. Animals in group I consumed water only without nicotine and then were intravenously administrated with PBS buffer (5 ml/kg). Animals in group II were kept in cages with supplements of nicotine-containing water and also received intravenous injections of PBS. Animals in group III were provided nicotine-containing water and intravenously received α9 BsAb (0.42 mg/kg) through tail vein injection once a week. On day 14, the mice were sacrificed and Matrigel plugs were collected for further studies. The Matrigel plugs were photographed under a dissecting microscope for visual analysis. The formation of new blood vessels in the Matrigel plugs was quantified by measuring the hemoglobin concentration.

Cyanmethemoglobin method

To evaluate the angiogenic response, the cyanmethemoglobin method was performed to measure the hemoglobin concentration in the Matrigel plugs. The Matrigel plugs were homogenized in 500 µl lysis solution containing 0.1% Brij-35 and incubated overnight at 4 °C. The hemoglobin concentration in the samples was measured using a Drabkin reagent kit (Sigma-Aldrich) according to the manufacturer's protocol [34]. Optical density at 540 nm was measured in a microplate reader, and final hemoglobin concentrations were calculated in accordance with hemoglobin standards.

Statistical analysis

Statistical analyses were performed using GraphPad Prism 5 software (GraphPad Software Inc.), with results presented as mean ± SD. A one-way analysis of variance (ANOVA) followed by Tukey's post hoc test was applied to determine statistical significance between groups. The probability value (p-value) of less than 0.05 was considered indicative of statistical significance.

Results

Anti-α9-nAChR bispecific antibody inhibited nicotine-induced α9-nAChR expression in triple-negative breast cancer cells

Our results indicated that nicotine at 10 µM induced significant α9-nAChR expression in mRNA and proteins (Fig. 1A–C), which was consistent with previous studies showing that nicotine induced the expression of α9-nAChRs in breast cancer cells [32]. To confirm nicotine-induced mRNA and protein expression of α9-nAChR, mRNA and protein were harvested from MDA-MB-231 cells exposed to nicotine at concentrations of 0.1, 1, 10 and 100 µM for 48 h, followed by mRNA and protein quantification were analyzed by real-time PCR and the western blotting analysis, respectively. The results showed

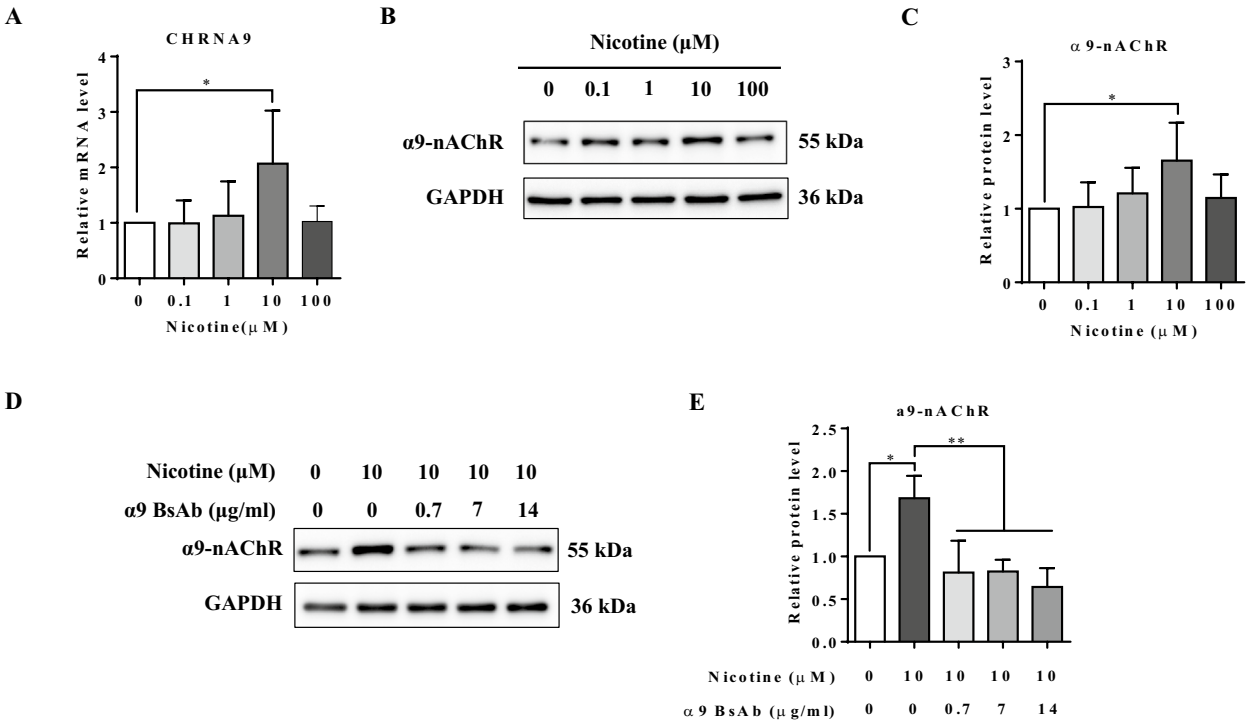

Fig. 1 The nicotine-induced increased expression of a9-nAChR in MDA-MB-231 was abrogated by α9 BsAb. The relative CHRNA9 mRNA expression of MDA-MB-231 cells exposed to nicotine at concentrations of 0.1, 1, 10 and 100 μM for 48 h (**A**). The nicotine-induced α9-nAChR protein expression at various concentrations for 72 h was measured using western blotting (**B**) and (**C**). The expression of α9-nAChR protein in α9 BsAb-pretreated MDA-MB-231 cells exposed to 10 μM nicotine (**D**) and (**E**). The values are calculated as mean ± SE of three independent experiments. *$p < 0.05$; **$p < 0.01$

that nicotine at 10 μM statistically significantly induced CHRNA9 mRNA expression in MDA-MB-231 cells with a 2.2-fold increase compared to the cells without exposure to nicotine (Fig. 1A). We also noticed nicotine at 10 μM increased the protein production of α9-nAChR in MDA-MB-231 cells with a 1.7-fold increase compared to the cells without exposure to nicotine (Fig. 1B and C), which is consistent with the results of nicotine-induced CHRNA9 mRNA expression. These results indicated that 10 μM of nicotine is the optimal concentration for inducing α9-nAChR expression in triple-negative breast cancer cells in our study, which is consistent with previous studies [35, 36].

To evaluate the antagonistic effect of anti-α9-nAChR bispecific antibody (α9 BsAb) and the role of α9-nAChR in nicotine-induced α9-nAChR expression, we pretreated the cells with α9 BsAb at concentrations of 0.7, 7, 14 μg/ml for 30 min and then exposed to 10 μM nicotine for 72 h. The result indicated that α9 BsAb at 0.7, 7, 14 μg/ml inhibited nicotine-induced α9-nAChR protein production, suggesting α9 BsAb exhibited the antagonistic characteristics toward α9-nAChR and abrogated nicotine-induced α9-nAChR expression in MDA-MB-231 cells (Fig. 1D and E).

The α9-nAChR expressed on endothelium and breast cancer cells played an important role in nicotine-induced angiogenesis

It has been demonstrated that α9-nAChRs, but not α7 subunits, contribute to retinal vascular development and ischemia-induced retinal neovascularization (NV) in mice with ischemic retinopathy [37]. This suggests the α9-nAChR may play a role in angiogenesis. In contrast, another study found that α7-nAChRs, but not α9-nAChR subunits, mediate migration, survival, proliferation and tube formation of human dermal microvascular endothelial cells (HMVECs) [38]. These two contradictory findings on the role of nAChR subunits in nicotine-mediated angiogenesis attracted our attention to unbraid the role of α9-nAChR in angiogenesis.

It has been reported that α9-nAChRs are highly expressed, particularly in HMVECs and human umbilical vein endothelial cells (HUVECs) [38]. Therefore, in this study, we aimed to investigate the role of α9-nAChRs in nicotine-mediated angiogenesis in HUVECs. To assess the role of α9-nAChRs in angiogenesis, we first performed tube formation assays with HUVECs. HUVECs were cultured in Endothelial Cell Growth Medium supplemented with 10 μM nicotine and α9 BsAb at concentrations of 0.7, 7 or 14 μg/ml

for 8 h and tubulogenesis was observed. The results showed that it appeared the elongated shape and formed more loops in HUVECs exposed to nicotine compared to the cells without exposure to nicotine (control group), whereas the numbers of loops were decreased in the cells exposed to medium with the addition of α9 BsAb in a dose-dependent manner, suggesting α9 BsAb inhibited nicotine-induced tubular formation of HUVECs (Fig. 2A and B).

In addition, we also proposed that nicotine-treated cancer cells may release either particular cytokines, growth factors or both to regulate migration, proliferation and tube formation of HUVECs, resulting in promoting angiogenesis in tumor surrounding tissue. To examine our hypothesis, cell supernatants were harvested and collected from the culture medium of MDA-MB-231 cells pre-incubated without or with 0.7, 7 and 14 μg/ml α9 BsAb for 30 min followed by re-supplement of 10 μM nicotine containing medium for an additional 72-h culture time. In order to investigate the role of supernatant from MDA-MB-231 cell culture medium, we prepared the conditioned medium (CM) at 50:50 volume ratio of cancer cell supernatant and endothelial cell growth medium for the tube formation assessment of HUVECs. Then, HUVECs were incubated in various combinations of CM for 8 h to observe the differences in tube formation. The results indicated the CM containing the supernatant from nicotine-exposed MDA-MB-231 cells increased the number of loops compared to the CM containing the supernatant from MDA-MB-231 cells without exposure to nicotine (control group). As CM containing the supernatant from cells exposed to α9 BsAb, however, the number of loops was statistically significantly decreased and this decrease was positively proportional to α9 BsAb concentrations in MDA-MB-231 culture medium (Fig. 2C and D). This indicated that the supernatant from nicotine-treated MDA-MB-231 cells induced tube formation of ECs, but α9 BsAb impaired this supernatant-induced enhancement of tube formation, suggesting that α9 BsAb may inhibit the production or secretion of pro-angiogenic factors in MDA-MB-231 cells. In

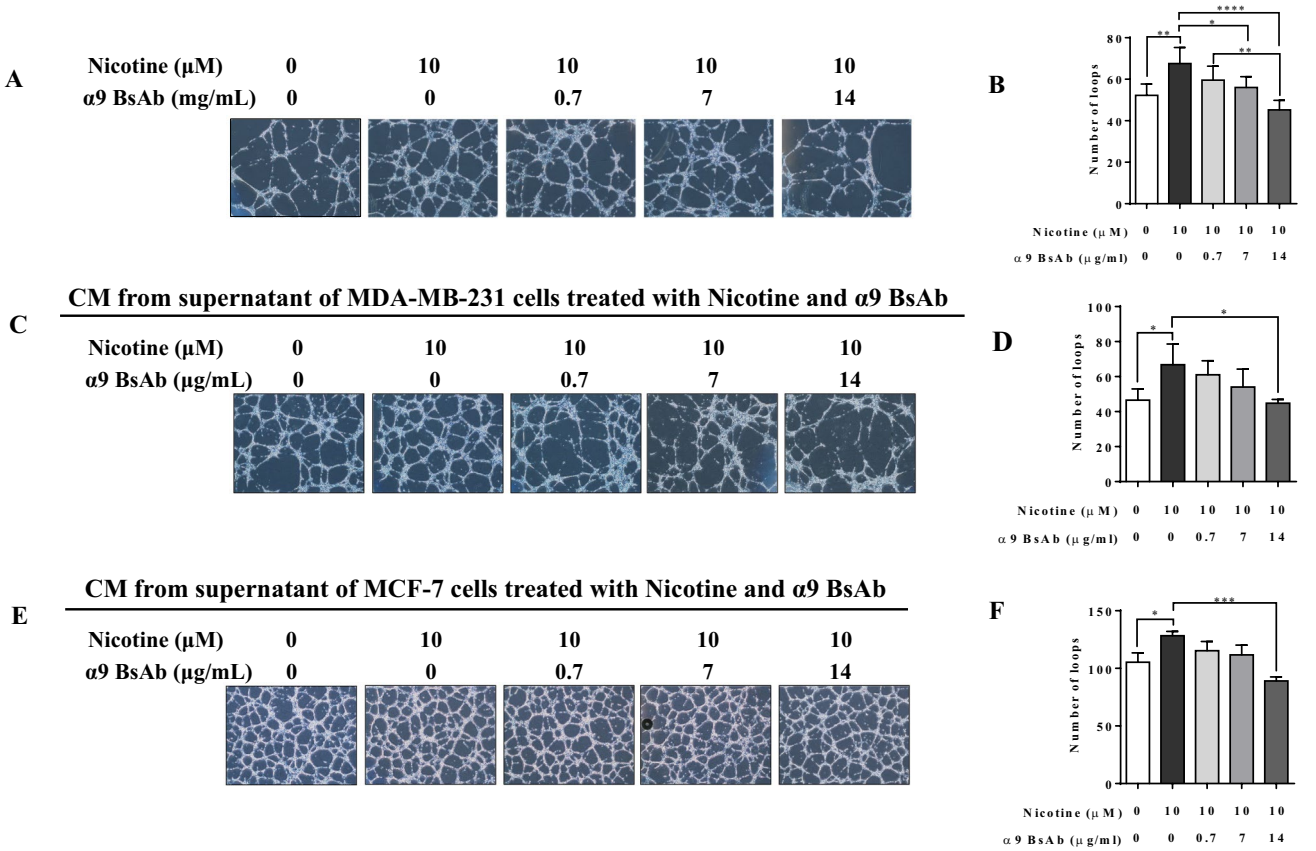

Fig. 2 The α9 BsAb against α9-nAChR reduced the number of loops in EC tube formation assay. The image (**A**) and quantification data (**B**) showed the number of nicotine-mediated loops in the endothelial cells treated with 10 μM nicotine and α9 BsAb at concentrations of 0.7, 7 or 14 μg/ml for 8 h. The conditioned medium containing the supernatant from nicotine-exposed MDA-MB-231 cell culture medium (**C** and **D**) and MCF-7 cell culture medium (**E** and **F**) increased HUVEC tube formation, while nicotine-induced this effect was impaired when HUVECs were incubated with the conditioned medium containing the supernatant of α9 BsAb treated cells. The values are calculated as mean ± SE for at least three independent experiments. *$p < 0.05$; **$p < 0.01$; ***$p < 0.001$; ****$p < 0.0001$

addition to MDA-MB-231 cells, we also tested in another α9-nAChR positive cell line MCF-7 whether it also exhibits this nicotine-induced production of pro-angiogenic factors and acts as the paracrine-like pattern on angiogenesis or not. The results indicated in Fig. 2E and F showed a similar outcome in MCF-7 as we observed in the results of tube formation assay using MDA-MB-231 cells under the same experimental procedure and protocol. It demonstrated that nicotine not only directly activated α9-nAChRs on ECs to promote angiogenesis but also worked on α9-nAChRs of breast cancer cells to trigger and release the angiogenic factors in regulating or promoting angiogenesis of the adjacent ECs.

The role of α9-nAChR on nicotine-induced angiogenesis was assessed using in vivo Matrigel plug assay and the microtube array membranes (MTAMs) murine models

The Matrigel plug assay for in vivo evaluation of angiogenesis was performed in 7–8 week-old NSG mice. MDA-MB-231 cells were infused into the cold liquid matrigel, following subcutaneous injection into the right flank of mice, solidification allowed to recruit ECs and form a new microvascular network. To evaluate the role of α9-nAChR on nicotine-induced angiogenesis in triple-negative breast cancers, phosphate-buffered saline (PBS) (PBS + 0.05% BSA; 5 ml/kg) or α9 BsAb (0.42 mg/kg) was intravenously administrated into animals once in a week. To increase the angiogenic potential in mice, mice were received nicotine (200 μg/ml) in their drinking water for 2 weeks. On the 14th day after Matrigel implantation, Matrigel plugs were removed and photographed for quantitative analysis. The schematic diagram is illustrated in Fig. 3A. These resected Matrigel plugs from mice received different treatments appeared differently from light to dark red, as shown in Fig. 3B. To quantify the amount of newly formed blood vessels in the plugs, we first homogenized these Matrigel plugs with Drabkin's solution for hemoglobin estimation and the quantitative results were presented in Fig. 3C. It was found that the average hemoglobin concentration in Matrigel plugs from mice received only PBS was 40.25 mg/ml, while it gained more than a three-fold increase and reached 137.125 mg/ml in mice consumed nicotine-containing drinking water. However, the hemoglobin concentration was significantly decreased to 81.5 mg/ml in nicotine-exposed mice received intravenous administration of α9 BsAb. Again, this also suggested that nicotine-induced angiogenesis occurred in α9-nAChR-dependent manner.

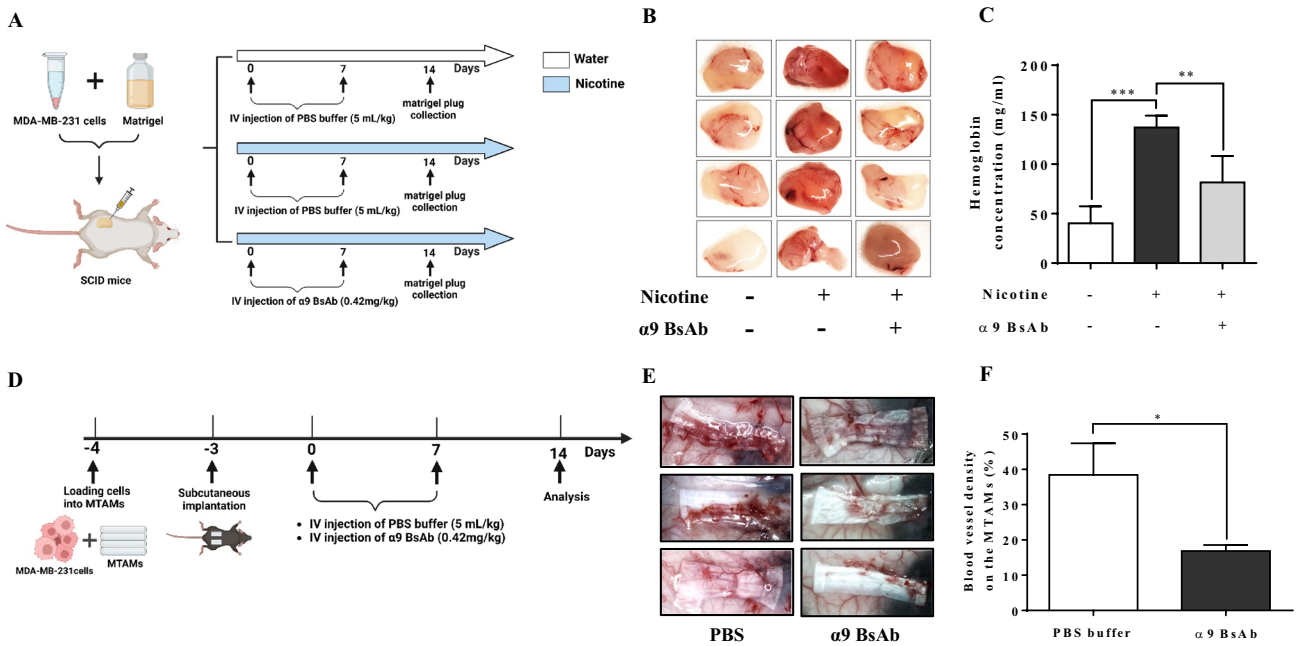

Fig. 3 The in vivo assessment of nicotine-induced angiogenesis in Matrigel Plug Assay and MTAM murine model. A schematic diagram for the experimental schedule of the in vivo Matrigel plug assay (**A**). Representative macroscopic images of explanted Matrigel plugs taken on day 14 after implantation (magnification, × 200) (**B**). Quantification of hemoglobin levels in Matrigel plugs (**C**). A schematic diagram for the experimental schedule of the microtube array membranes (MTAMs) murine models (**D**). Anti-angiogenic effect of α9 BsAb in MTAM murine model (**E**) and (**F**). The values are calculated as mean ± SE for at least three independent experiments. *$p < 0.05$; **$p < 0.01$; ***$p < 0.001$

To confirm our findings, a novel in vivo drug screening platform of the microtube array membranes (MTAMs) was used to assess the role of α9-nAChRs in angiogenesis. In brief, 1×10^6 MDA-MB-231 cells were loaded into MTAMs and then placed in the medium for 24 h. The cell-loaded MTAMs were then implanted subcutaneously into wild C57BL/6 immunocompetent mice labeled as day 1. MTAM-implanted mice were intravenously injected with PBS (5 ml/kg) or α9 BsAb (0.42 mg/kg) weekly. On day 14, MTAMs were surgically removed from the sacrificed mice for angiogenesis assessment. The schematic diagram is illustrated in Fig. 3D. Compared with the control group received PBS treatment, a significant reduction in vascular development was observed on implanted MTAM of mice with the administration of α9 BsAb (Fig. 3E). The quantitative analysis of vascular development was analyzed using Image J image analysis software and the results are shown in Fig. 3F, indicating that systemic administration of the α9-nAChR antagonist α9 BsAb inhibited angiogenesis in the MDA-MB-231-loaded MTAM mice. This in vivo evaluation for angiogenesis was consistent with the results we observed in the Matrigel plug assay.

The nicotine induced VEGF-A, VEGFR2 and phosphorylated VEGFR2 expression through the α9-nAChR activation

Since it has been demonstrated that vascular endothelial growth factors (VEGFs) are responsible for new blood vessel formation during embryo development, ischemia injury and angiogenesis, we aimed to determine the expression of VEGFs in nicotine-treated MDA-MB-231 cells. We measured the mRNA and protein expressions of VEGF-A in cells exposed to nicotine only or combination of nicotine and α9 BsAb. The results indicated that nicotine-induced VEGF-A mRNA expression was positively correlated to the concentration of nicotine and it reached the optimal production of mRNA of VEGF-A from cells exposed to 10 μM nicotine, which was near to twofold increase compared to control (without exposure to nicotine) (Fig. 4A). We also measured the expression of the other forms of VEGFs, including VEGF-B and VEGF-C, in cells treated with either medium containing 10 μM nicotine only or supplemented with 14 μg/mL α9 BsAb. The result revealed that only mRNA expression of VEGF-A was elevated by nicotine and this nicotine-induced increased mRNA expression of VEGF-A

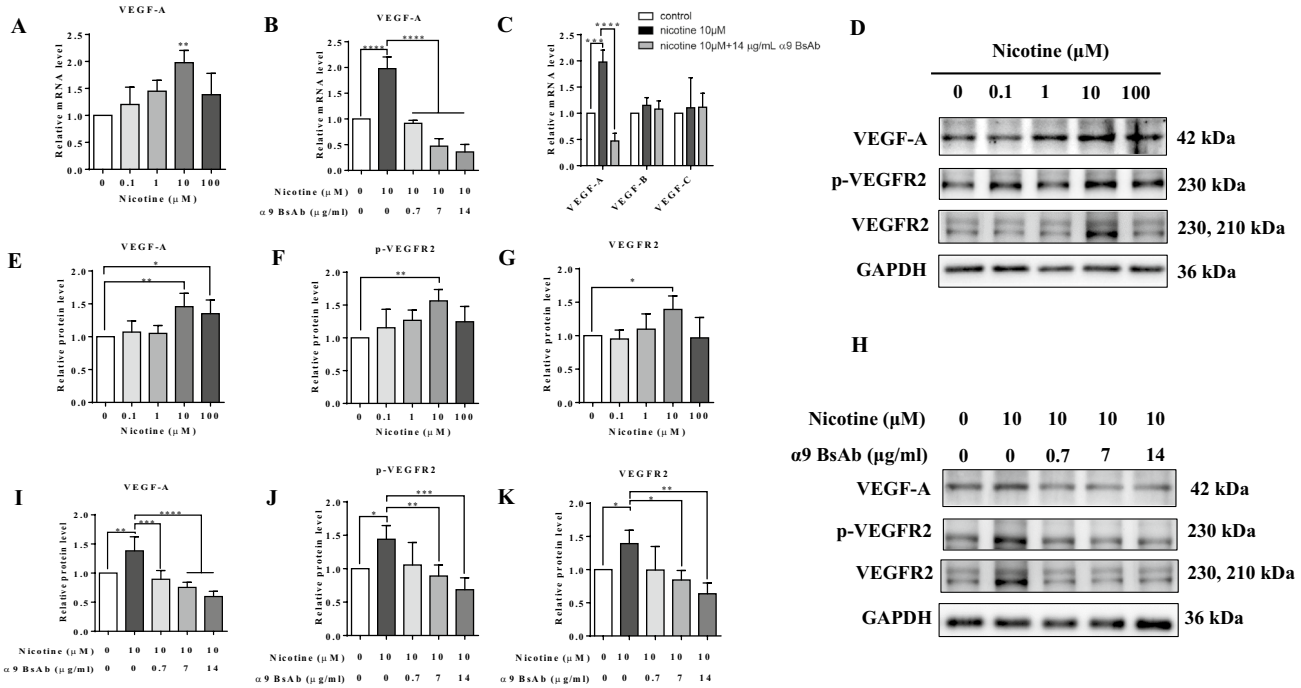

Fig. 4 The expressions of VEGF-A, p-VEGFR2 and VEGFR2 mRNA and protein in MDA-MB 231 cells treated with nicotine. The expression of VEGF-A mRNA levels in MDA-MB-231 cells treated with increasing concentrations of nicotine for 48 h (**A**). The mRNA expression of VEGF-A (**B**) and its variants (**C**) levels in MDA-MB-231 cells following nicotine and α9 BsAb treatment. The expression of VEGF-A, VEGFR-2 and p-VEGFR-2 protein levels in MDA-MB-231 cells treated with nicotine concentrations from 0.1, 1, 10 and 100 μM for 72 h (**D**–**G**). The expression of VEGF-A, VEGFR-2 and p-VEGFR-2 proteins in MDA-MB-231 cells pretreated with α9 BsAb at 0.7, 7, 14 μg/ml for 30 min followed by exposure to 10 μM nicotine for 72 h (**H**–**K**). The values are calculated as mean ± SE for at least three independent experiments. *$p < 0.05$; **$p < 0.01$; ***$p < 0.001$

was blocked by α9 BsAb (Fig. 4C). We also found that α9 BsAb-mediated inhibitory effect on mRNA expression of VEGF-A was observed in MDA-MB-231 cells exposed to nicotine and this inhibitory degree was positively correlated to the α9 BsAb concentration, suggesting that α9-nAChR played an important role in nicotine-mediated VEGF-A mRNA expression (Fig. 4B). Moreover, we also measured the protein level of VEGF-A to confirm the results acquired from the α9 BsAb-mediated reduction of VEGF-A mRNA. The results showed that nicotine at concentrations of 10 and 100 μM increased the expression of VEGF-A protein (Fig. 4D and E). Nicotine at 10 μM also boosted the production of VEGFR2 and phosphorylated VEGFR2 (p-VEGFR2) proteins by western blotting analysis (Fig. 4D, F and G). To investigate the role of α9-nAChR in nicotine-mediated downstream signaling in the elevated production of VEGF-A, VEGFR2 and p-VEGFR2, we examined the expression of VEGF-A, VEGFR2 and p-VEGFR2 proteins in MDA-MB-231 cells pretreated with α9 BsAb at 0.7, 7, 14 μg/ml for 30 min followed by exposure to 10 μM nicotine for 72 h. The results indicated that MDA-MB-231 cells pretreated with α9 BsAb displayed a reduction in nicotine-induced expression of VEGF-A, VEGFR2 and p-VEGFR2 proteins (Fig. 4H) and this α9 BsAb-mediated reduction appeared as in a dose-dependent manner (Fig. 4I–K). Collectively, our results suggest that nicotine activated α9-nAChR coupled with triggering the downstream signaling to increase expression of VEGF-A, VEGFR2 and p-VEGFR2 in MDA-MB-231 cells for promoting angiogenesis, migration and proliferation.

A significant reduction in the expression of VEGF-A, VEFGFR2 and p-VEGFR2 of MDA-MB-231 cells pre-treated with α9 shRNA

To confirm our findings, three stable α9-nAChR-knockdown cell lines were selected using α9 shRNA in MDA-MB-231 cells. This α9-nAChR shRNA-mediated reduction of α9-nAChR was evaluated by measuring the expression levels of α9-nAChR mRNA and protein using real-time polymerase chain reaction (RT-PCR) and the western blotting, respectively. The results showed all of three stains exhibited a significant reduction of α9-nAChR mRNA and proteins (Fig. 5A and B), indicating that we succeeded in generating three α9-nAChR deficient MDA-MB-231 cell lines. The clone sh-nAChR9 #2 displayed the most significant inhibitory effect on the production of α9-nAChR protein among these three clones. Therefore, we compared the expression of VEGF-A, VEGFR2 and p-VEGFR2 between MDA-MB-231 and sh-nAChR9 #2 clone. As shown in Fig. 5C, the expression of VEGF-A, VEFGR2 and p-VEGFR2 was reduced in the sh-nAChR9 #2 clone. Moreover, nicotine failed to reboot the VEGF-A, VEFGR2 and p-VEGFR2 production in the sh-nAChR9 #2 clone (Fig. 5C), suggesting both α9 BsAb and α9 shRNA against α9-nAChR exhibited the antagonistic activity to α9-nAChRs.

Detections of the pro-angiogenic factor in conditioned medium from nicotine-exposed MDA-MB-231 cell supernatant

To uncover the pro-angiogenic factor in conditioned medium from nicotine-exposed MDA-MB-231 cells, we examined the expression level of VEGF in the supernatant of MDA-MB-231 cell culture medium. MDA-MB-231 cells were treated with nicotine at concentrations of 0.1, 1, 10

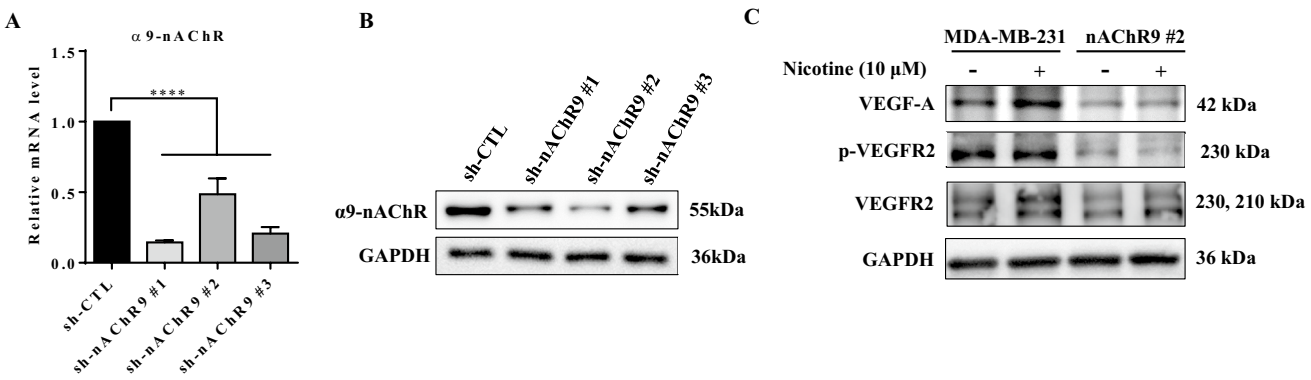

Fig. 5 The expression levels of α9-nAChR, VEGF-A, VEGFR2 and p-VEGFR2 after transfection of shRNA-nAChR9 in MDA-MB-231 cells. The expression of α9-nAChR mRNA (**A**) and protein (**B**) levels in MDA-MB-231 cells transfected with CHRNA9-specific shRNA. The expression of VEGF-A, p-VEGFR2 and VEGFR2 protein levels in MDA-MB-231 cells with or without transfection of shRNA-nAChR9 after nicotine treatment (**C**). The values are calculated as mean ± SE of three independent experiments. ****$p < 0.0001$

and 100 μM for 72 h. The conditioned medium was then collected for quantitative measurements of VEGF using Enzyme-Linked Immunosorbent Assay (ELISA). The result shown in Fig. 4A revealed that nicotine at 10 μM significantly increased VEGF release to the supernatant of MDA-MB-231 cells (Fig. 6A). To evaluate the role of α9-nAChR in VEGF release in the supernatant, MDA-MB-231 cells were first treated with α9 BsAb at 0.7, 7 and 14 μg/ml before exposure to 10 μM nicotine. Compared to VEGF level in conditioned medium derived from the cells only exposed to nicotine, the VEGF secretion was significantly decreased and displayed in a dose-dependent inhibitory manner (Fig. 6B). It suggested that VEGF-containing conditioned medium from nicotine-exposed MDA-MB-231 cells modulated endothelial tube-forming activities through the paracrine signaling pattern.

The nicotine-α9-nAChR signaling axis triggered the increased expressions of HIF-2α and MMP9 in MDA-MB-231 cells

The expression of VEGFs is regulated by various factors such as hypoxia, pH, growth factors and cytokines [39, 40]. Under hypoxic conditions, for example, the transcription factor hypoxia-inducible factor-2α (HIF-2α) is transported into the nucleus where it binds to HIF-1β. This complex interacts with a specific sequence on the VEGF gene called the hypoxia response element (HRE), leading to trigger VEGF gene transcription and then VEGF protein is produced and secreted from the cancer cells [41]. Therefore, we carried out western blotting analysis to examine whether nicotine induces HIF-2α expression through the activation of the α9-nAChR in MDA-MB-231 cells. Our results presented in Fig. 7A and B showed that nicotine at 10 μM enhanced HIF-2α expression in MDA-MB-231 cells. However, pretreatment of α9 BsAb impaired nicotine-induced HIF-2α expression of MDA-MB-231 cells. In addition, we also evaluated the role of nicotine in modulating the expression of matrix metalloproteinase2 (MMP2) and matrix metalloproteinase9 (MMP9) which are enzymes for enzymatically hydrolyzing the type IV collagen of basement membrane. The results indicated that nicotine induced the expression of MMP9 expression in MDA-MB-231 cells and this nicotine-induced increased MMP9 expression was blocked when cells were pretreated with α9 BsAb. The image data from western blotting and their quantitative data were indicated as in Fig. 7A and C. But, no difference was observed in the expression of MMP2 protein levels between control and nicotine-treated groups (Fig. 7A and D). Again, it suggested nicotine induced HIF-2α and MMP9 expression through α9-nAChRs. It has been suggested that MMP9 is associated with cell migration and invasion [42]. Therefore, we evaluated the migration and invasive effects of nicotine on MDA-MB-231 cells using Transwell Assays. The results revealed nicotine increased cell migration and invasion of MDA-MB-231 cells. Again, nicotine-mediated increase in migration and invasion were blocked by α9 BsAb (Fig. 7E–G).

Discussion

This study revealed, for the first time, the pro-angiogenic role of α9-nAChRs in nicotine-mediated angiogenesis in triple-negative breast cancers. To investigate the role of α9-nAChRs in nicotine-mediated angiogenesis, we used the novel special bispecific monoclonal antibody as a

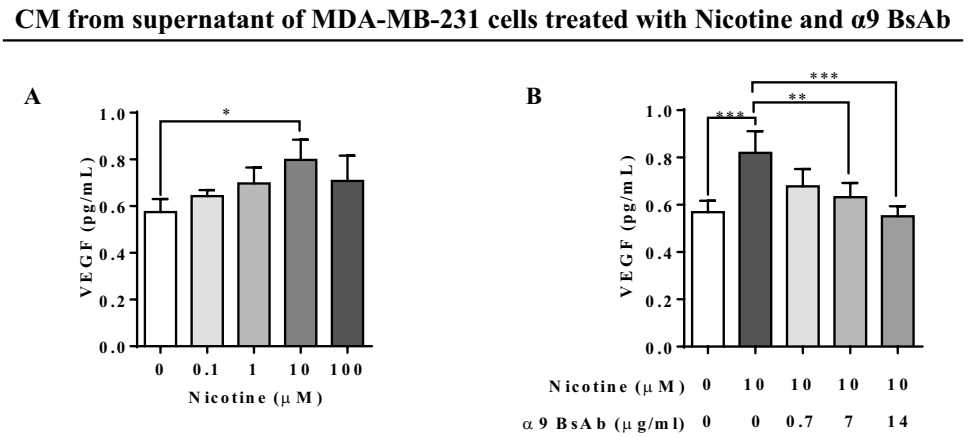

Fig. 6 The presence of Vascular Endothelial Growth Factor (VEGF) in culture supernatant of MDA-MB-231 cells. The VEGF production in the CM from the supernatant of MDA-MB-231 cells cultured in a serum-free medium containing increasing concentrations of nicotine for 72 h (**A**). α9 BsAb inhibits nicotine-induced VEGF production in the supernatant of MDA-MB-231 cell nicotine-containing culturing medium (**B**). The values are calculated as mean ± SE of four independent experiments. *p < 0.05; **p < 0.01; ***p < 0.001

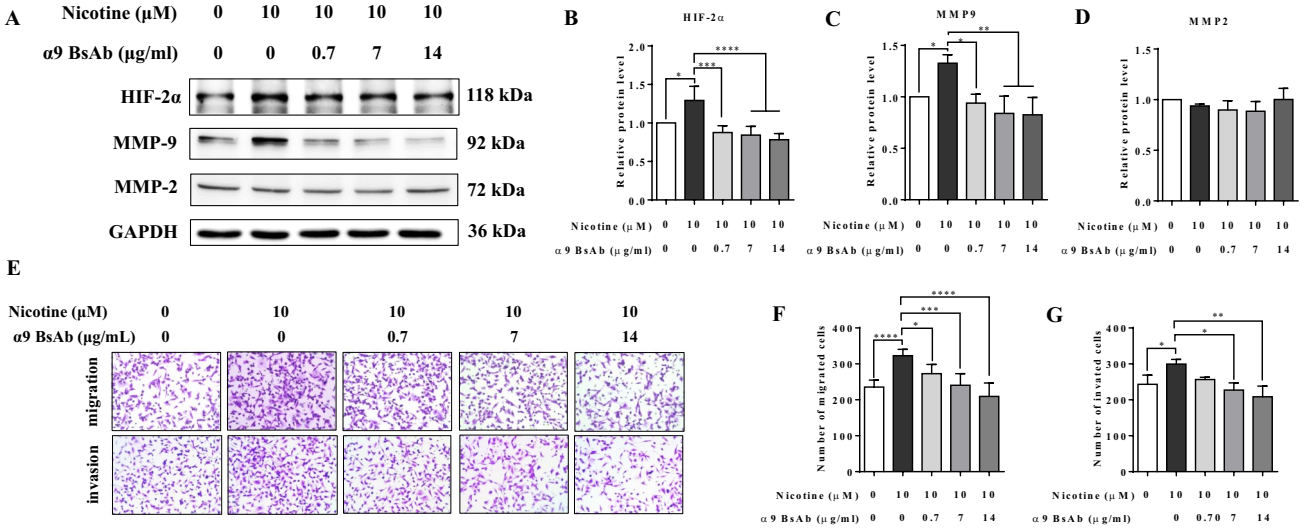

Fig. 7 The expression of HIF-2α, MMP2 and MMP9 protein in MDA-MB-231 cells exposed to nicotine. The detections of HIF-2α, MMP2 and MMP9 protein using Immunoblotting (**A**) and the quantitative analysis (**B**) and (**C**) showed *α9* BsAb inhibits nicotine-induced HIF-2α and MMP9 protein expressions of MDA-MB-231 cells. Nicotine failed to increase MMP2 expression from MDA-MB-231 cells (**A** and **D**). The images in the migration and invasive assessments using Transwell assays (**E**). The quantitative assessment of cell migration and invasion indicated nicotine increased migration and invasion of MDA-MB-231 cells and this nicotine-mediated enhancement in migration and invasion was blocked by α9 BsAb (**F**) and (**G**). The values are calculated as mean ± SE for at least three independent experiments. *$p < 0.05$; **$p < 0.01$; ***$p < 0.001$; ****$p < 0.0001$

selective α9-nAChR antagonist against α9-nAChRs and then confirmed the results using the stable knockdown of α9-nAChR expression in MDA-MB-231 cells. In addition to α7-nAChRs [43], we demonstrated nicotine-induced angiogenesis through activations of α9-nAChRs in the tube formation assay, MTAM angiogenic assessment, and Matrigel plug assay in the murine model.

Nicotine is an angiogenic factor that stimulates endogenous cholinergic signaling pathways to promote angiogenesis. Recently, it has been described that nicotine at 10 μM was shown to induce the transformation in normal breast epithelial cells and proliferation of breast cancer cells [27]. It has been revealed that nicotine induces the expression of α9-nAChRs in human breast cancer cells [44, 45]. Consistent with previous findings, we also demonstrated that nicotine at 10 μM significantly increased the mRNA and protein expressions of α9-nAChR in MDA-MB-231 cells in Fig. 1. Moreover, the bispecific monoclonal antibody (α9 BsAb) inhibited nicotine-induced α9-nAChR expression, suggesting this newly developed α9 BsAbs were an effectively competitive antagonist of nicotine to α9-nAChR. This bispecific monoclonal antibody (α9 BsAb) consists of one arm of Fab fragment against mPEG, which is a molecule on the surface of mPEGylated nanomedicine (i.e., PLD), and the other arm of single chain variable fragment (scFv) against α9-nAChR antigen, which is overexpressed on triple-negative breast cancer cells. To characterize the angiogenic role of α9-nAChR in breast cancers in this study, α9 BsAb without any therapeutic conjugations was used.

The endothelial cell tube formation assay is considered as a rapid and quantitative method for determining proteins or pathways involved in angiogenesis [46, 47]. We found nicotine and supernatants from nicotine-exposed MDA-MB-231 or MCF-7 cell culture medium significantly induced an increased number of loop formation in tube formation assay. However, α9 BsAb blocked both nicotine- and supernatants-induced loop formation of endothelial cells, suggesting α9-nAChR played an important role in nicotine-mediated angiogenesis. Although we demonstrated the pro-angiogenetic role of α9-nAChR in the in vitro angiogenesis assay, we wanted to confirm this observation in the in vivo murine models, including the Matrigel plug assay [48–50] and MTAM murine platform. These results indicated nicotine increases the hemoglobin contents in the subcutaneously implanted Matrigel in murine, but this effect is blocked by α9 BsAb. MTAM was originally designed as an in vivo cell culture platform, subcutaneously implanted into immunocompetent mice [50]. It has been applied to assess the proliferation and angiogenesis of adenocarcinoma human alveolar basal epithelial cells (A549 cells) in wild-type Balb/C mice [51]. We demonstrated that α9 BsAb inhibited blood vessel formation on the MTAM membrane by more than 50% reduction, compared with control mice without exposure to α9 BsAb. All three in vitro and in vivo angiogenesis assessments indicated α9-nAChRs were mediated

with nicotine-induced angiogenesis. It was the first report correlated to the previous studies by Sean F. Hackett et al. research group, indicating the deletion of α9-nAChR was associated with the reduced retinal neovascularization in the murine OIR model [37].

To decipher the molecular mechanism of nicotine-α9-nAChRs axis signaling, we investigated and quantified mRNA and protein expression of several key angiogenic mediators in cells using reverse transcription polymerase chain reaction (RT-PCR) and western blotting. VEGFs and their receptors (VEGFRs) have been recognized as one of the principal initiators in regulating tumor angiogenesis. VEGF-A binds to and activates both VEGFR-1 and VEGFR-2, promoting angiogenesis, vascular permeability, cell migration, survival, proliferation and gene expression in endothelial cells of blood vessels [52, 53]. In addition, VEGF secreted from cancer cells also binds to the VEGFRs on their own cell surface, triggering signaling to stimulate their own growth and survival [4, 8, 17, 54]. Previous studies have shown that nicotine-induced expression of growth factors such as VEGFs and their counterpart receptors is one of the major molecular mechanisms underlying the pro-angiogenic effects of nAChRs in several types of cancers [25, 26]. In agreement with previous studies, our results showed that nicotine exposure stimulated the expression of VEGF-A, VEGFR2 and p-VEGFR2 and increased VEGF secretion in MDA-MB-231 cells. The increased expression of these proteins was inhibited by α9 shRNA targeting α9-nAChRs and a selective α9-nAChR antagonist (α9 BsAb), suggesting that nicotine-induced α9-nAChR activation followed by an increased expression and activations of VEGF and VEGFRs in triple-negative breast cancer cells. We also noticed that nicotine at 10 μM induced an increased expression of VEGF-A (~ 34%) in triple-negative breast cancer cells (BT549) and then this nicotine-induced VEGF-A production was blocked by α9 BsAb at dosage ≥ 7 μg/mL (see Supplementary Fig. 1). Hypoxia-inducible factors (HIFs) are a heterodimer complex consisting of an oxygen-dependent α-subunit (HIF-α) and an oxygen-independent β-subunit (HIF-β). As cellular oxygen levels decrease, this heterodimer binds to hypoxia-responsive elements (HREs) within the promoter of hypoxia-responsive target genes including those involved in angiogenesis and cell proliferation such as vascular endothelial growth factor (VEGF), VEGF receptors, platelet-derived growth factor B (PDGF-B) and matrix metalloproteinases (MMP2 and MMP9) [55, 56]. HIF-2α, one of the HIF-α, is commonly upregulated in a variety of human tumors, including breast cancer [57]. According to the investigation from Alexandra et al., overexpression of HIF-2α is associated with increased vascular density and increased metastatic capacity in breast cancer patients [58]. Shaima Salman et al., also investigated that nicotine exposure leads to a slow, progressive accumulation of HIF-2α through the activation of α7-nAChR [59]. In this study, we revealed that nicotine exposure induced HIF-2α expression through interaction with α9-nAChR in MDA-MB-231 cells. MMPs, particularly gelatinases, contribute to angiogenesis by degrading basement membrane and other ECM components, allowing endothelial cells to migrate into the tumor and develop new blood vessels [1, 60]. Gelatinase A (MMP2) and gelatinase B (MMP9) differ from other MMPs because of their ability to degrade gelatin and type IV collagen, the main component of the basement membrane, which is the main barrier separating in situ and invasive carcinoma [61]. A few studies have shown that MMP2 positivity is associated with an unfavorable prognosis in both premenopausal and postmenopausal node-positive breast carcinoma patients [62–64], while few others have suggested that MMP2 negativity may be linked with a favorable prognosis in node-negative breast carcinoma [65]. Moreover, Coussens et al. and Bergers et al. reported that MMP9 is important for angiogenesis in tumor xenograft models [66, 67]. Although the precise mechanism remains unknown, MMP9 acts by increasing the bioavailability of the pro-angiogenic factor (VEGF). Surprisingly, MMP2 was not required to induce angiogenesis in murine model [67]. These findings indicate that MMP9 is more facilitated in promoting tumor growth through induction of angiogenesis than MMP2. In line with previous studies, our results showed that nicotine exposure did not make a difference in MMP2 expression in MDA-MB-231 cells, while it increased MMP9 expression and nicotine-induced increased MMP9 expression was inhibited by α9 BsAb, suggesting that α9-nAChR plays an important role in regulating nicotine-induced MMP9 expression. In addition, a significant reduction in MMP9 expression was observed in an α9-nAChR stable knockdown MDA-MB-231 cells, compared to controls (see Supplementary Fig. 2). Moreover, α9 BsAb also impaired the activities of migration and invasion of MDA-MB-231 cells in the transwell assays, suggesting the nicotine-α9-nAChR-MMP9 signaling axis impacts on angiogenesis.

In summary, our findings indicated that nicotine induced α9-nAChR activation and then triggered the production of HIF-2α, VEGF-A, VEGFR2, p-VEGFR2 and MMP9 in MDA-MB-231 cells. In addition, increased VEGF secretion from the nicotine-exposed cancer cells could bind to VEGFR2 on their own surface as well as the receptors on endothelial cells, allowing proliferating cancer cells and prolonging their survival, meanwhile promoting angiogenesis of endothelial cells in tumor microenvironments and increasing gap junction of endothelial cell layers [68–70] (Fig. 8). This nicotine-induced angiogenic effect was blocked by our novel bispecific antibody (α9 BsAb) in triple-negative breast cancer.

In conclusion, our findings suggest that α9-nAChR plays a critical role in nicotine-induced angiogenesis and

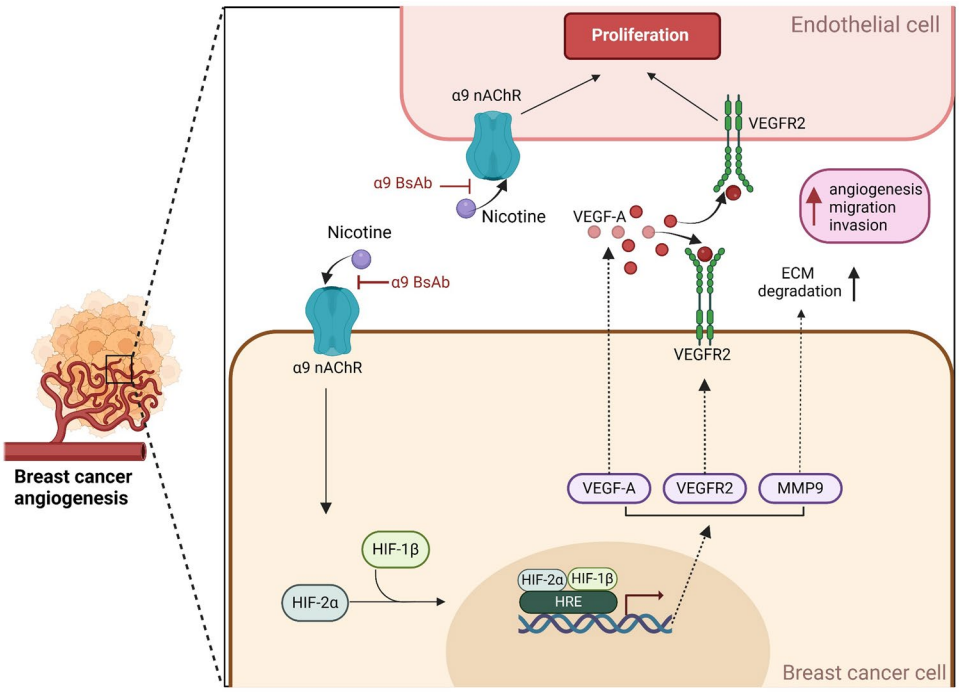

Fig. 8 Proposed signaling pathway of α9-nAChR in nicotine-induced triple-negative breast cancer angiogenesis

this bispecific antibody (α9 BsAb) may serve as a potential therapeutic candidate for treatments of the α9 positive cancers such as triple-negative breast cancers and other types of human mammary adenocarcinoma.

Nicotine binds and interacts with α9-nAChR on the surface of MDA-MB-231 cells, triggering signaling in activating HIF-2α, increasing expression of VEGF-A, VEGFR2, p-VEGFR2 and MMP9. The elevated VEGF-A may simultaneously modulate the activities of cancer and endothelial cells. VEGF secreted from cancer cells can bind to the VEGFR2 on their own surface, proliferating cancer cells to growth and survival, appearing as an internal autocrine VEGF loop pattern in regulating their own activities. Moreover, it may bind to VEFGR2 receptors on endothelial cells and then promote angiogenesis. However, α9 BsAb inhibits nicotine-induced angiogenic effects in triple-negative breast cancer.

Supplementary Information The online version contains supplementary material available at https://doi.org/10.1007/s10456-024-09944-6.

Acknowledgements We would like to express our gratitude to BioRender used to make summary figure in this study.

Author contributions Conceptualization, SO and JC; methodology, SO, T-CK, T-HH and MC; software, SO, T-CK and T-HH; validation, SO, T-CK, T-HH and JC; formal analysis, SO; investigation, SO, T-CK, T-HH; resources, K-HC, C-CC and C-CC; data curation, SO, T-CK; writing—original draft preparation, SO, C-CH and JC; writing—review and editing, SR and JC; visualization, T-CK; supervision, JC; project administration, JC; funding acquisition, JC. All authors have read and agreed to the published version of the manuscript.

Funding This work was supported by Taipei Medical University Hospital (103TMUH-WFH-02–3), Ministry of Science and Technology, Taiwan (MOST104-2314-B-038–062), and the Health and Welfare Surcharge of Tobacco Products grant (MOHW110-TDU-B-212–144014), awarded to Jungshan Chang.

Data availability No datasets were generated or analysed during the current study.

Declarations

Competing interests The authors declare no competing interests.

References

1. Lugano R, Ramachandran M, Dimberg A (2020) Tumor angiogenesis: causes, consequences, challenges and opportunities. Cell Mol Life Sci 77(9):1745–1770
2. Behelgardi MF et al (2020) Targeting signaling pathways of VEGFR1 and VEGFR2 as a potential target in the treatment of breast cancer. Mol Biol Rep 47(3):2061–2071
3. Takahashi H, Shibuya M (2005) The vascular endothelial growth factor (VEGF)/VEGF receptor system and its role under physiological and pathological conditions. Clin Sci (Lond) 109(3):227–241
4. Chung AS, Lee J, Ferrara N (2010) Targeting the tumour vasculature: insights from physiological angiogenesis. Nat Rev Cancer 10(7):505–514
5. Zhang S et al (2017) Immunoglobulin-like domain 4-mediated ligand-independent dimerization triggers VEGFR-2 activation in HUVECs and VEGFR2-positive breast cancer cells. Breast Cancer Res Treat 163(3):423–434

6. Jinesh GG et al (2017) Surface PD-L1, E-cadherin, CD24, and VEGFR2 as markers of epithelial cancer stem cells associated with rapid tumorigenesis. Sci Rep. https://doi.org/10.1038/s41598-017-08796-z
7. Luo M et al (2016) VEGF/NRP-1axis promotes progression of breast cancer via enhancement of epithelial-mesenchymal transition and activation of NF-kappaB and beta-catenin. Cancer Lett 373(1):1–11
8. Zhao D et al (2015) VEGF drives cancer-initiating stem cells through VEGFR-2/Stat3 signaling to upregulate Myc and Sox2. Oncogene 34(24):3107–3119
9. Zhu X, Zhou W (2015) The emerging regulation of VEGFR-2 in triple-negative breast cancer. Front Endocrinol (Lausanne) 6:159
10. Riquelme E et al (2014) VEGF/VEGFR-2 upregulates EZH2 expression in lung adenocarcinoma cells and EZH2 depletion enhances the response to platinum-based and VEGFR-2-targeted therapy. Clin Cancer Res 20(14):3849–3861
11. Lu-Emerson C et al (2015) Lessons from anti-vascular endothelial growth factor and anti-vascular endothelial growth factor receptor trials in patients with glioblastoma. J Clin Oncol 33(10):1197–1213
12. Mahfouz N et al (2017) Gastrointestinal cancer cells treatment with bevacizumab activates a VEGF autoregulatory mechanism involving telomerase catalytic subunit hTERT via PI3K-AKT, HIF-1alpha and VEGF receptors. PLoS ONE 12(6):e0179202
13. Zhong ZY et al (2017) Circular RNA MYLK as a competing endogenous RNA promotes bladder cancer progression through modulating VEGFA/VEGFR2 signaling pathway. Cancer Lett 403:305–317
14. Pengcheng S et al (2017) MicroRNA-497 suppresses renal cell carcinoma by targeting VEGFR-2 in ACHN cells. Biosci Rep. https://doi.org/10.1042/BSR20170270
15. Jang K et al (2017) VEGFA activates an epigenetic pathway upregulating ovarian cancer-initiating cells. EMBO Mol Med 9(3):304–318
16. Liu KS et al (2017) Apatinib promotes autophagy and apoptosis through VEGFR2/STAT3/BCL-2 signaling in osteosarcoma. Cell Death Dis 8:e3015
17. Perrot-Applanat M, Di Benedetto M (2012) Autocrine functions of VEGF in breast tumor cells: adhesion, survival, migration and invasion. Cell Adh Migr 6(6):547–553
18. Heeschen C et al (2001) Nicotine stimulates angiogenesis and promotes tumor growth and atherosclerosis. Nat Med 7(7):833–839
19. Heeschen C et al (2002) A novel angiogenic pathway mediated by non-neuronal nicotinic acetylcholine receptors. J Clin Invest 110(4):527–536
20. Albuquerque EX et al (2009) Mammalian nicotinic acetylcholine receptors: from structure to function. Physiol Rev 89(1):73–120
21. Fasoli F, Gotti C (2015) Structure of neuronal nicotinic receptors. Curr Top Behav Neurosci 23:1–17
22. Le Novere N, Corringer PJ, Changeux JP (2002) The diversity of subunit composition in nAChRs: evolutionary origins, physiologic and pharmacologic consequences. J Neurobiol 53(4):447–456
23. Govind AP, Walsh H, Green WN (2012) Nicotine-induced upregulation of native neuronal nicotinic receptors is caused by multiple mechanisms. J Neurosci 32(6):2227–2238
24. Brown KC et al (2013) Nicotine induces the up-regulation of the alpha7-nicotinic receptor (alpha7-nAChR) in human squamous cell lung cancer cells via the Sp1/GATA protein pathway. J Biol Chem 288(46):33049–33059
25. Shi D et al (2012) Nicotine promotes proliferation of human nasopharyngeal carcinoma cells by regulating alpha7AChR, ERK, HIF-1alpha and VEGF/PEDF signaling. PLoS ONE 7(8):e43898
26. Ma X et al (2014) alpha5 Nicotinic acetylcholine receptor mediates nicotine-induced HIF-1alpha and VEGF expression in non-small cell lung cancer. Toxicol Appl Pharmacol 278(2):172–179
27. Lee CH et al (2010) Overexpression and activation of the alpha9-nicotinic receptor during tumorigenesis in human breast epithelial cells. J Natl Cancer Inst 102(17):1322–1335
28. Sun Z et al (2020) Differential expression of nicotine acetylcholine receptors associates with human breast cancer and mediates antitumor activity of alphaO-conotoxin GeXIVA. Mar Drugs 18(1):1–61
29. Singh S, Pillai S, Chellappan S (2011) Nicotinic acetylcholine receptor signaling in tumor growth and metastasis. J Oncol 2011:456743
30. Pucci S et al (2021) alpha9-containing nicotinic receptors in cancer. Front Cell Neurosci 15:805123
31. Huang LC et al (2017) Nicotinic acetylcholine receptor subtype alpha-9 mediates triple-negative breast cancers based on a spontaneous pulmonary metastasis mouse model. Front Cell Neurosci 11:336
32. Guha P et al (2014) Nicotine promotes apoptosis resistance of breast cancer cells and enrichment of side population cells with cancer stem cell-like properties via a signaling cascade involving galectin-3, alpha9 nicotinic acetylcholine receptor and STAT3. Breast Cancer Res Treat 145(1):5–22
33. Chen M et al (2021) A novel anti-tumor/anti-tumor-associated fibroblast/anti-mPEG tri-specific antibody to maximize the efficacy of mPEGylated nanomedicines against fibroblast-rich solid tumor. Biomater Sci 10(1):202–215
34. Pintavirooj C et al (2021) Noninvasive portable hemoglobin concentration monitoring system using optical sensor for anemia disease. Healthcare (Basel) 9(6):647
35. Pucci S et al (2022) α9-containing nicotinic receptors in cancer. Front Cell Neurosci. https://doi.org/10.3389/fncel.2021.805123
36. Guha P et al (2014) Nicotine promotes apoptosis resistance of breast cancer cells and enrichment of side population cells with cancer stem cell-like properties via a signaling cascade involving galectin-3, α9 nicotinic acetylcholine receptor and STAT3. Breast Cancer Res Treat 145(1):5–22
37. Hackett SF et al (2017) The nicotinic cholinergic pathway contributes to retinal neovascularization in a mouse model of retinopathy of prematurity. Invest Ophthalmol Vis Sci 58(2):1296–1303
38. Wu JC et al (2009) Cholinergic modulation of angiogenesis: role of the 7 nicotinic acetylcholine receptor. J Cell Biochem 108(2):433–446
39. Chen L, Endler A, Shibasaki F (2009) Hypoxia and angiogenesis: regulation of hypoxia-inducible factors via novel binding factors. Exp Mol Med 41(12):849–857
40. Elias AP, Dias S (2008) Microenvironment changes (in pH) affect VEGF alternative splicing. Cancer Microenviron 1(1):131–139
41. Poon E, Harris AL, Ashcroft M (2009) Targeting the hypoxia-inducible factor (HIF) pathway in cancer. Expert Rev Mol Med 11:e26
42. Hong OY et al (2022) Inhibition of cell invasion and migration by targeting matrix metalloproteinase-9 expression via sirtuin 6 silencing in human breast cancer cells. Sci Rep. https://doi.org/10.1038/s41598-022-16405-x
43. Cooke JP, Ghebremariam YT (2008) Endothelial nicotinic acetylcholine receptors and angiogenesis. Trends Cardiovasc Med 18(7):247–253
44. Lee CH et al (2011) Crosstalk between nicotine and estrogen-induced estrogen receptor activation induces α9-nicotinic acetylcholine receptor expression in human breast cancer cells. Breast Cancer Res Treat 129(2):331–345
45. Tu SH et al (2011) Tea polyphenol (-)-epigallocatechin-3-gallate inhibits nicotine- and estrogen-induced alpha9-nicotinic acetylcholine receptor upregulation in human breast cancer cells. Mol Nutr Food Res 55(3):455–466

46. Arnaoutova I et al (2009) The endothelial cell tube formation assay on basement membrane turns 20: state of the science and the art. Angiogenesis 12(3):267–274
47. Kubota Y et al (1988) Role of laminin and basement-membrane in the morphological-differentiation of human-endothelial cells into capillary-like structures. J Cell Biol 107(4):1589–1598
48. Cattaneo MG et al (2003) Alprostadil suppresses angiogenesis in vitro and in vivo in the murine Matrigel plug assay. Br J Pharmacol 138(2):377–385
49. Kragh M et al (2003) In vivo chamber angiogenesis assay: an optimized Matrigel plug assay for fast assessment of anti-angiogenic activity. Int J Oncol 22(2):305–311
50. Aref Z, Quax PHA (2021) In vivo Matrigel plug assay as a potent method to investigate specific individual contribution of angiogenesis to blood flow recovery in mice. Int J Mol Sci 22(16):8909
51. Huang WT et al (2022) Microtube array membrane hollow fiber assay (MTAM-HFA)-an accurate and rapid potential companion diagnostic and pharmacological interrogation solution for cancer immunotherapy (PD-1/PD-L1). Biomolecules 12(4):480
52. Shibuya M (2011) Vascular endothelial growth factor (VEGF) and its receptor (VEGFR) signaling in angiogenesis: a crucial target for anti- and pro-angiogenic therapies. Genes Cancer 2(12):1097–1105
53. Abhinand CS et al (2016) VEGF-A/VEGFR2 signaling network in endothelial cells relevant to angiogenesis. J Cell Commun Signal 10(4):347–354
54. Momeny M et al (2017) Anti-tumour activity of tivozanib, a pan-inhibitor of VEGF receptors, in therapy-resistant ovarian carcinoma cells. Sci Rep. https://doi.org/10.1038/srep45954
55. Krock BL, Skuli N, Simon MC (2011) Hypoxia-induced angiogenesis: good and evil. Genes Cancer 2(12):1117–1133
56. Rankin EB, Giaccia AJ (2008) The role of hypoxia-inducible factors in tumorigenesis. Cell Death Differ 15(4):678–685
57. Helczynska K et al (2008) Hypoxia-inducible factor-2alpha correlates to distant recurrence and poor outcome in invasive breast cancer. Cancer Res 68(22):9212–9220
58. Giatromanolaki A et al (2006) Hypoxia-inducible factor-2 alpha (HIF-2 alpha) induces angiogenesis in breast carcinomas. Appl Immunohistochem Mol Morphol 14(1):78–82
59. Salman S, Brown ST, Nurse CA (2012) Chronic nicotine induces hypoxia inducible factor-2alpha in perinatal rat adrenal chromaffin cells: role in transcriptional upregulation of KATP channel subunit Kir6.2. Am J Physiol Cell Physiol 302(10):C1531-8
60. Quintero-Fabian S et al (2019) Role of matrix metalloproteinases in angiogenesis and cancer. Front Oncol 9:1370
61. Duffy MJ et al (2000) Metalloproteinases: role in breast carcinogenesis, invasion and metastasis. Breast Cancer Res 2(4):252–257
62. Talvensaari-Mattila A et al (2001) Matrix metalloproteinase-2 (MMP-2) is associated with the risk for a relapse in postmenopausal patients with node-positive breast carcinoma treated with anti-estrogen adjuvant therapy. Breast Cancer Res Treat 65(1):55–61
63. Talvensaari-Mattila A, Paakko P, Turpeenniemi-Hujanen T (1999) MMP-2 positivity and age less than 40 years increases the risk for recurrence in premenopausal patients with node-positive breast carcinoma. Breast Cancer Res Treat 58(3):287–293
64. Talvensaari-Mattila A et al (1998) Matrix metalloproteinase-2 immunoreactive protein: a marker of aggressiveness in breast carcinoma. Cancer 83(6):1153–1162
65. Hirvonen R et al (2003) Matrix metalloproteinase-2 (MMP-2) in T(1–2)N0 breast carcinoma. Breast Cancer Res Treat 77(1):85–91
66. Coussens LM et al (2000) MMP-9 supplied by bone marrow-derived cells contributes to skin carcinogenesis. Cell 103(3):481–490
67. Bergers G et al (2000) Matrix metalloproteinase-9 triggers the angiogenic switch during carcinogenesis. Nat Cell Biol 2(10):737–744
68. Conklin BS et al (2002) Nicotine and cotinine up-regulate vascular endothelial growth factor expression in endothelial cells. Am J Pathol 160(2):413–418
69. Lee TH et al (2003) Vascular endothelial growth factor modulates the transendothelial migration of MDA-MB-231 breast cancer cells through regulation of brain microvascular endothelial cell permeability. J Biol Chem 278(7):5277–5284
70. Natori T et al (2003) Nicotine enhances neovascularization and promotes tumor growth. Mol Cells 16(2):143–146

Publisher's Note Springer Nature remains neutral with regard to jurisdictional claims in published maps and institutional affiliations.

Springer Nature or its licensor (e.g. a society or other partner) holds exclusive rights to this article under a publishing agreement with the author(s) or other rightsholder(s); author self-archiving of the accepted manuscript version of this article is solely governed by the terms of such publishing agreement and applicable law.

Authors and Affiliations

Sonjid Ochirbat[1] · Tzu-Chun Kan[2,3] · Chun-Chun Hsu[2,4,5] · Tzu-Hsuan Huang[2,6] · Kuo-Hsiang Chuang[7] · Michael Chen[7] · Chun-Chia Cheng[8] · Chun-Chao Chang[9,10,11] · Sri Rahayu[12] · Jungshan Chang[1,2,13]

✉ Jungshan Chang
js.chang@tmu.edu.tw

[1] International Ph.D. Program in Medicine, College of Medicine, Taipei Medical University, Taipei 11031, Taiwan

[2] Graduate Institute of Medical Sciences, College of Medicine, Taipei Medical University, Taipei 11031, Taiwan

[3] Genomics Research Center, Academia Sinica, Taipei 115, Taiwan

[4] School of Respiratory Therapy, College of Medicine, Taipei Medical University, Taipei 11031, Taiwan

[5] Division of Pulmonary Medicine, Department of Internal Medicine, Taipei Medical University Hospital, Taipei 11031, Taiwan

[6] Department of Medical Research, Shuang Ho Hospital, Taipei Medical University, New Taipei City 23561, Taiwan

[7] Graduate Institute of Pharmacognosy, Taipei Medical University, Taipei 11031, Taiwan

[8] Research Center of Radiation Medicine, Chang Gung University, Taoyuan 33302, Taiwan

[9] Division of Gastroenterology and Hepatology, Department of Internal Medicine, Taipei Medical University Hospital, Taipei 11031, Taiwan

[10] Division of Gastroenterology and Hepatology, Department of Internal Medicine, School of Medicine, College of Medicine, Taipei Medical University, Taipei 11031, Taiwan

[11] TMU Research Center for Digestive Medicine, Taipei Medical University, Taipei 11031, Taiwan

[12] Department of Biology, Faculty of Mathematics and Natural Science, Universitas Negeri Jakarta, Jakarta 13220, Indonesia

[13] International Ph.D. Program for Cell Therapy and Regeneration Medicine, College of Medicine, Taipei Medical University, Taipei 11031, Taiwan